Supporting Information

Synthesis and luminescence properties of two silver cluster-assembled materials for selective Fe^{3+} sensing

Jin Sakai,[a,‡] *Sourav Biswas,*[a,‡] *Tsukasa Irie,*[a] *Haruna Mabuchi,*[a] *Taishu Sekine,*[a] *Yoshiki Niihori,*[b] *Saikat Das*[b,*] *and Yuichi Negishi*[a,b,*]

[a]Department of Applied Chemistry, Faculty of Science, Tokyo University of Science, Kagurazaka, Shinjuku-ku, Tokyo 162-8601, Japan.

[b]Carbon Value Research Center, Research Institute for Science & Technology, Tokyo University of Science, Tokyo 162-8601, Japan

[‡]These authors contributed equally to this work.

*Corresponding Authors
S.D.: saikatdas@rs.tus.ac.jp
Y.N.: negishi@rs.tus.ac.jp

Table of Contents

Materials and methods

Materials

Unless otherwise indicated, all starting materials and solvents were purchased from commercial suppliers and used without further purification. 1,1,2,2-tetrakis(4-(pyridin-4-ylethynyl)phenyl)ethene (TPEPE) and 1,1,2,2-tetrakis(4-((E)-2-(pyridin-4-yl)vinyl)phenyl)ethene (TPVPE) were procured from ET Co., Ltd. Silver trifluoroacetate (CF_3COOAg) and other metal salts which were used for sensing measurements were obtained from FUJIFILM Wako Pure Chemical Corporation. $AgNO_3$, Acetonitrile, ethanol, tetrahydrofuran, dichloromethane were obtained from Kanto Chemical Co., Inc.

Instrumentation

The single crystals were immersed in Parabar 10312 oil based cryoprotectant (Hampton Research, 34 Journey, Aliso Viejo, CA 92656-3317 USA), mounted on a Dual-Thickness MicroMounts™ (MiTeGen, LLC, Ithaca, NY, USA) and kept at 90 K during the single-crystal X-ray diffraction (SCXRD) data collection. The diffraction data for the single crystals were acquired on a Bruker D8 QUEST diffractometer using monochromated Mo-Kα radiation (λ = 0.71073 Å). The crystal structures were determined using Bruker APEX3[1] software package. Powder X-ray diffraction (PXRD) patterns were recorded on a Rigaku X-ray diffractometer with Cu Kα radiation (λ = 1.5418 Å) operated at 40 kV and 40 mA over the range of 2θ = 4 to 20° with a step size of 0.02° and scan speed of 0.134° per min. Scanning electron microscopy (SEM) images were obtained on a JEOL JSM-7001F/SHL field emission scanning electron microscope with accelerating voltage of 5 kV. The energy dispersive spectrum (EDS) was collected using the same SEM instrument at a voltage of 15 kV. Thermogravimetric analysis (TGA) of the SCAMs was carried out on a Bruker TG-DTA2010SA instrument in a nitrogen atmosphere from room temperature to 800 °C at a ramp rate of 10 °C min^{-1} and nitrogen flow rate of 50 mL min^{-1}. UV-Vis absorption spectra were obtained with a JASCO V-770 spectrophotometer. Photoluminescence (PL) spectra were recorded on an Edinburgh Instruments (EI) FLS1000 spectrofluorometer equipped with a continuous (450 W) xenon lamp. PL decay curves were recorded on a fluorescent lifetime spectrometer (FLS1000) based on a time-correlated single-photon counting (TCSPC) technique under the excitation of 375 nm or 475 nm picosecond laser. To investigate solid-state light emission, the samples were subjected to irradiation using AS-ONE SLUV-6 at a wavelength of 365 nm. X-ray photoelectron spectroscopy (XPS) spectra were collected by using a JPS-9-1-MC electron spectrometer (JEOL, Tokyo, Japan). X-rays from the Mg-Kα line (1253.6 eV) were used for excitation. All the binding energies were referenced to the neutral C 1s.

Synthesis methods

Synthesis of silver *tert*-butylthiolate (AgS^{t}Bu). AgS^{t}Bu was synthesized according to the previously published procedure[2,3]. Briefly, a mixture of silver nitrate (2.204 g, 12.8 mmol) and acetonitrile (30 mL) was stirred for 10 min in a 100 mL Erlenmeyer flask. 5 mL (44 mmol) of *tert*-butyl mercaptan was added to the mixture followed by stirring for 15 min. The white precipitate was collected by centrifugation, washed several times with methanol until the smell was gone and then with acetonitrile (1 × 40 mL). Finally, the solid was dried under vacuum overnight to yield a white powder of AgS^{t}Bu (yield = 90%).

Solution preparation for sensing

To prepare the stock solution, each metal salt was dissolved in distilled water at room temperature. Subsequently, the stock solution was further diluted with distilled water to obtain specific concentrations. During the sensing measurements, the diluted solutions were added to the cuvette, and the final concentrations were determined based on the volume present in the cuvette.

Table S1. Crystal data and structure refinement parameters of **TUS 1**.

Identification code	**TUS 1**
Empirical formula	$C_{234}H_{204}Ag_{24}F_{36}N_{12}O_{24}S_{12}$
CCDC number	2256626
Formula weight	7225.68
Temperature/K	273.15
Crystal system	trigonal
Space group	*R*-3*c*
a/Å	59.1396(19)
b/Å	59.1396(19)
c/Å	32.143(3)
α/°	90
β/°	90
γ/°	120
Volume/Å^3	97359(10)
Z	9
ρ_{calc}/g cm^{-3}	1.109
μ/mm^{-1}	1.168
F(000)	31752.0
Crystal size/mm^3	0.2 × 0.15 × 0.14
Radiation	MoKα (λ = 0.71073)
2Θ range for data collection/°	3.644 to 50.242
Index ranges	$-70 \leq h \leq 70$, $-70 \leq k \leq 66$, $-38 \leq l \leq 38$
Reflections collected	367620
Independent reflections	19291 [R_{int} = 0.1201, R_{sigma} = 0.0383]
Data/restraints/parameters	19291/3130/895
Goodness-of-fit on F^2	1.043
Final R indexes [I>=2σ (I)]	R_1 = 0.0794, wR_2 = 0.2372
Final R indexes [all data]	R_1 = 0.1197, wR_2 = 0.2813
Largest diff. peak/hole / e Å^{-3}	1.20/-1.12

Table S2. Crystal data and structure refinement parameters of **TUS 2**.

Identification code	**TUS 2**
Empirical formula	$C_{234}H_{228}Ag_{24}F_{36}N_{12}O_{24}S_{12}$
CCDC number	2256627
Formula weight	7249.87
Temperature/K	273.15
Crystal system	trigonal
Space group	*R*-3*c*
a/Å	58.313(2)
b/Å	58.313(2)
c/Å	32.365(2)
α/°	90
β/°	90
γ/°	120
Volume/Å^3	95310(10)
Z	9
ρ_{calc}/g cm^{-3}	1.137
μ/mm^{-1}	1.193
F(000)	31968.0
Crystal size/mm^3	0.2 × 0.15 × 0.14
Radiation	MoKα (λ = 0.71073)
2Θ range for data collection/°	3.696 to 50.074
Index ranges	$-69 \leq h \leq 69$, $-69 \leq k \leq 69$, $-38 \leq l \leq 38$
Reflections collected	357526
Independent reflections	18728 [R_{int} = 0.1143, R_{sigma} = 0.0367]
Data/restraints/parameters	18728/3071/916
Goodness-of-fit on F^2	1.025
Final R indexes [I>=2σ (I)]	R_1 = 0.0721, wR_2 = 0.2062
Final R indexes [all data]	R_1 = 0.1080, wR_2 = 0.2519
Largest diff. peak/hole / e Å^{-3}	1.57/-1.11

Table S3. Parameters obtained from time-correlated single-photon counting (TCSPC) measurement.

Sample	Component	τ (ns)	A	f
TUS 1	1	0.799	0.702	0.335
	2	3.733	0.298	0.665
TUS 2	1	1.061	0.847	0.587
	2	4.135	0.153	0.413

Fitting parameters for **TUS 1** and **TUS 2** are 1.1 and 1.2, respectively. τ is the lifetime of each individual component, A is the amplitude, and f determines the fractional population of each component.

Table S4. Spiking recovery result for Fe^{3+} sensing in real water by **TUS 1**.

Sample		Fe^{3+} found	Fe^{3+} Added (μM)	% Error in detection
TUS 1	Tap water	0.316 nM	1	0.08
			2	0.07
			3	0.10
TUS 1	River water	0.141 μM	1	0.12
			2	0.11
			3	0.12

Table S5. Spiking recovery result for Fe^{3+} sensing in real water by **TUS 2**.

Sample		Fe^{3+} found	Fe^{3+} Added (μM)	% Error in detection
TUS 2	Tap water	–	1	0.18
			2	0.18
			3	0.19
TUS 2	River water	0.126 μM	1	0.24
			2	0.21
			3	0.19

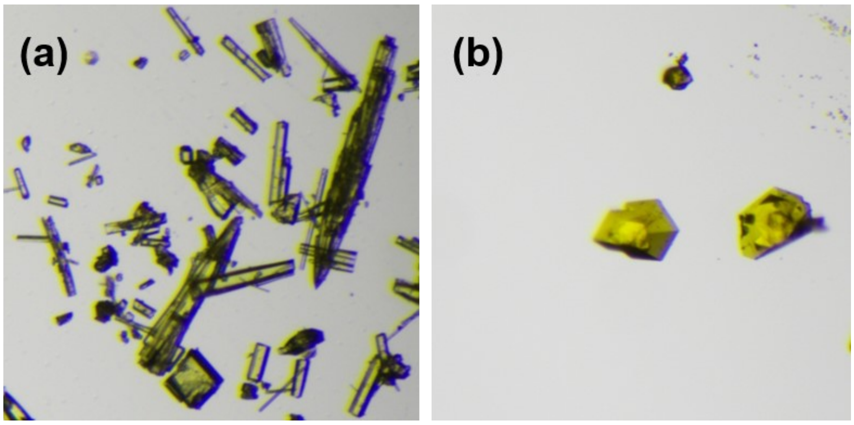

Fig. S1 Optical microscope images of (a) **TUS 1** and (b) **TUS 2**.

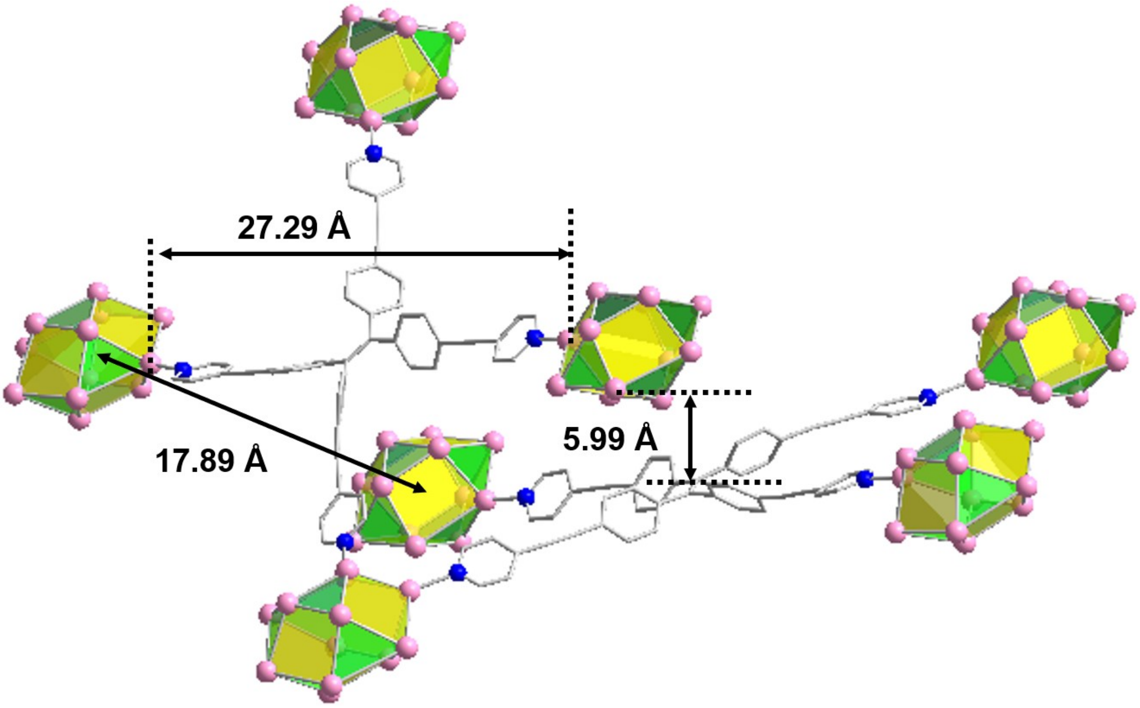

Fig. S2 Three-dimensional architectural parameters of **TUS 1**. Color legend: Ag, pink; N, blue C, grey stick; H atoms are omitted.

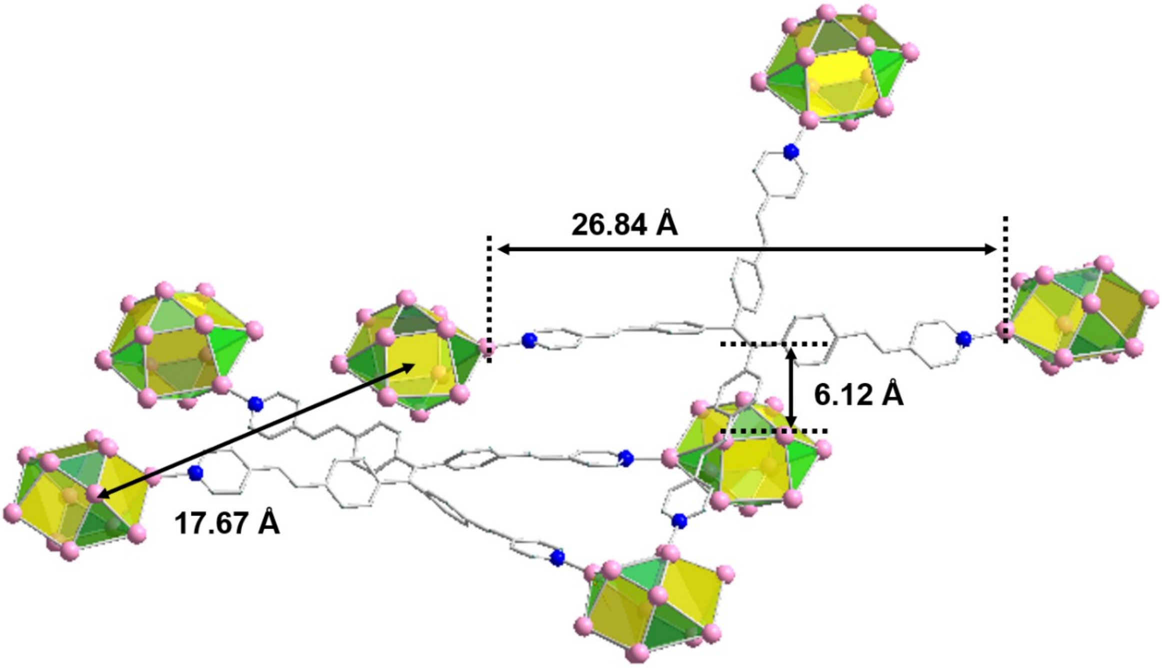

Fig. S3 Three-dimensional architectural parameters of **TUS 2**. Color legend: Ag, pink; N, blue C, grey stick; H atoms are omitted.

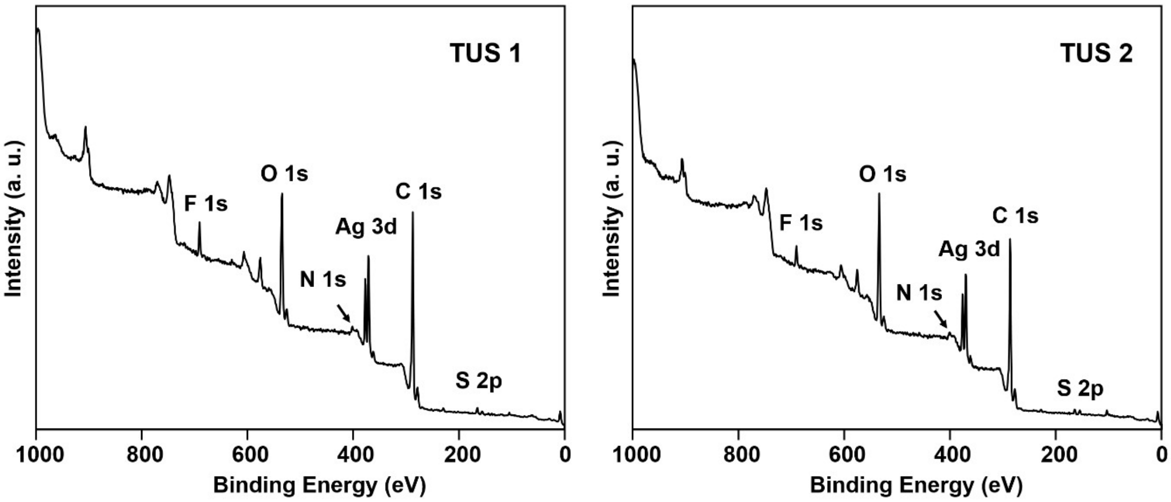

Fig. S4 XPS survey spectra of **TUS 1** and **TUS 2**.

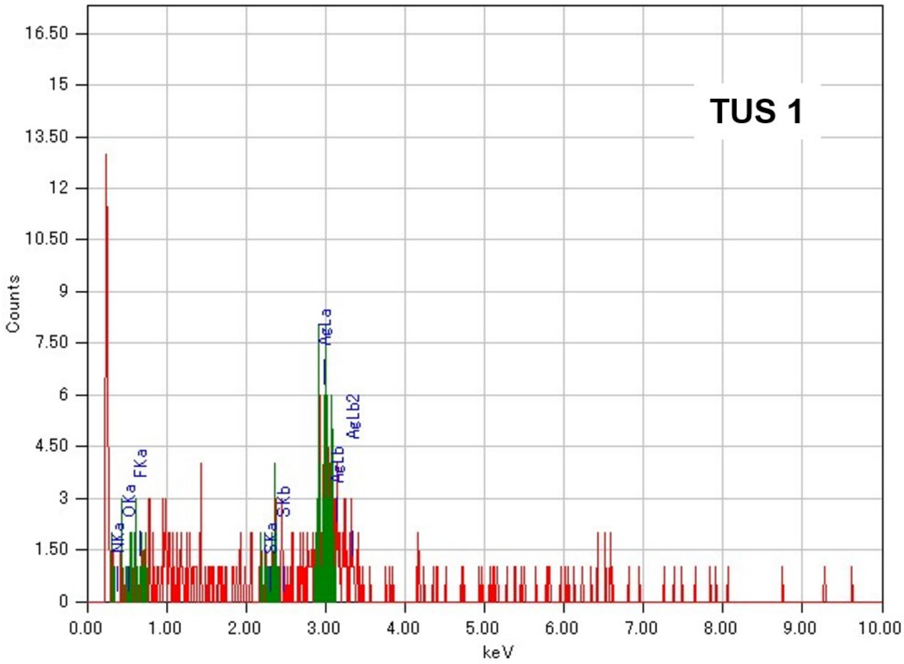

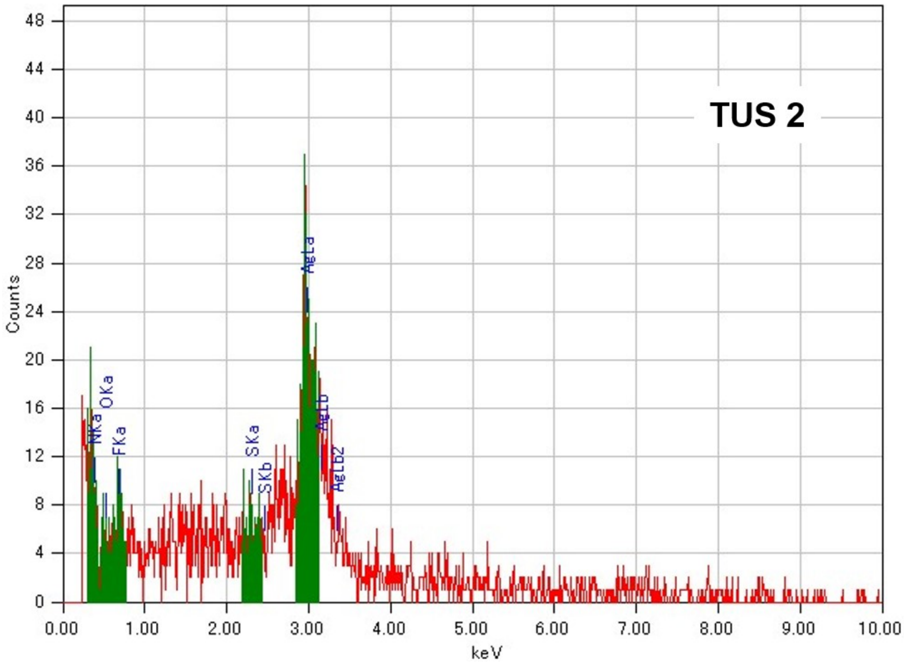

Fig. S5 EDS of both **TUS 1** and **TUS 2**.

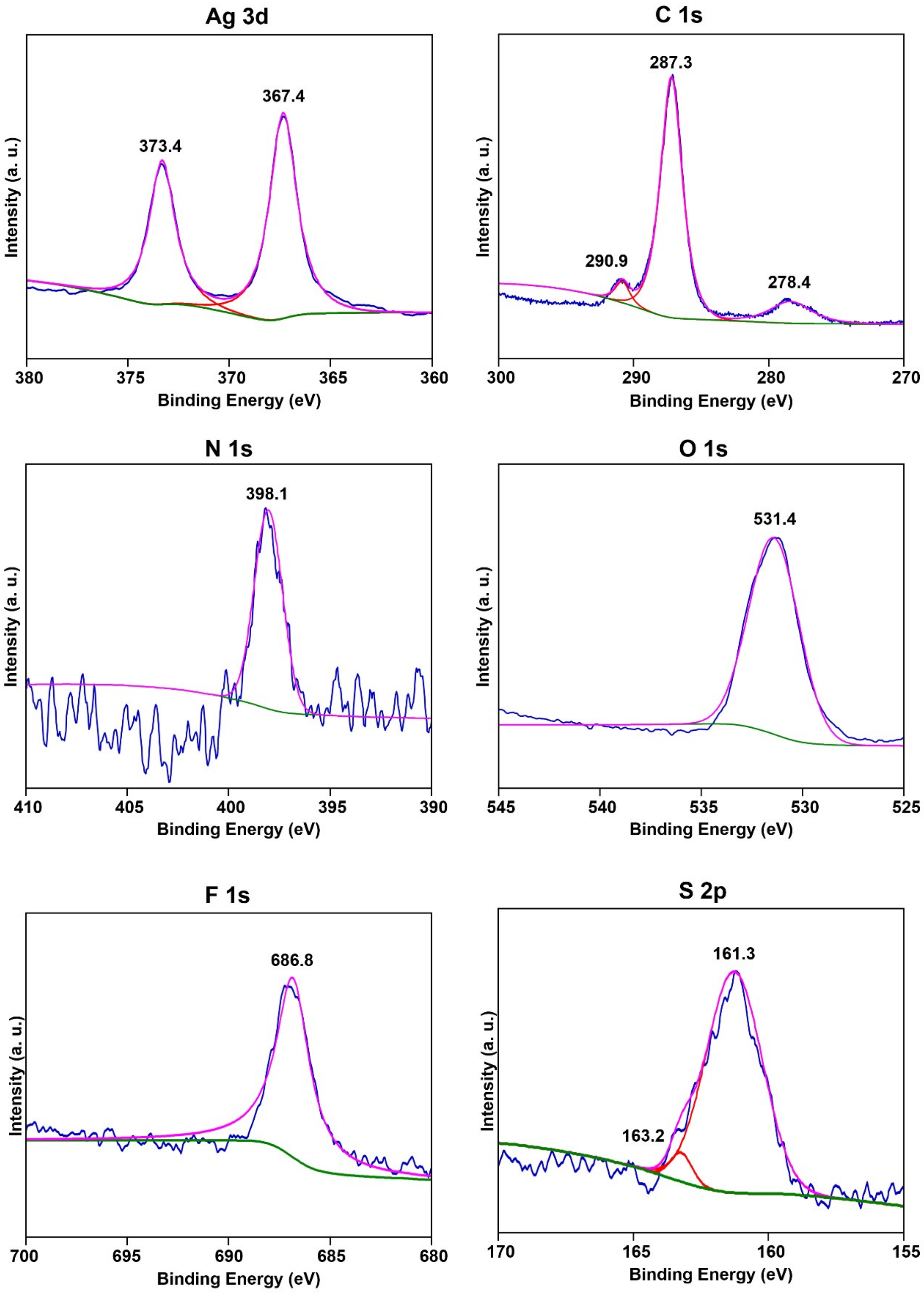

Fig. S6 High-resolution XPS binding energy spectrum of each element present in **TUS 1**.

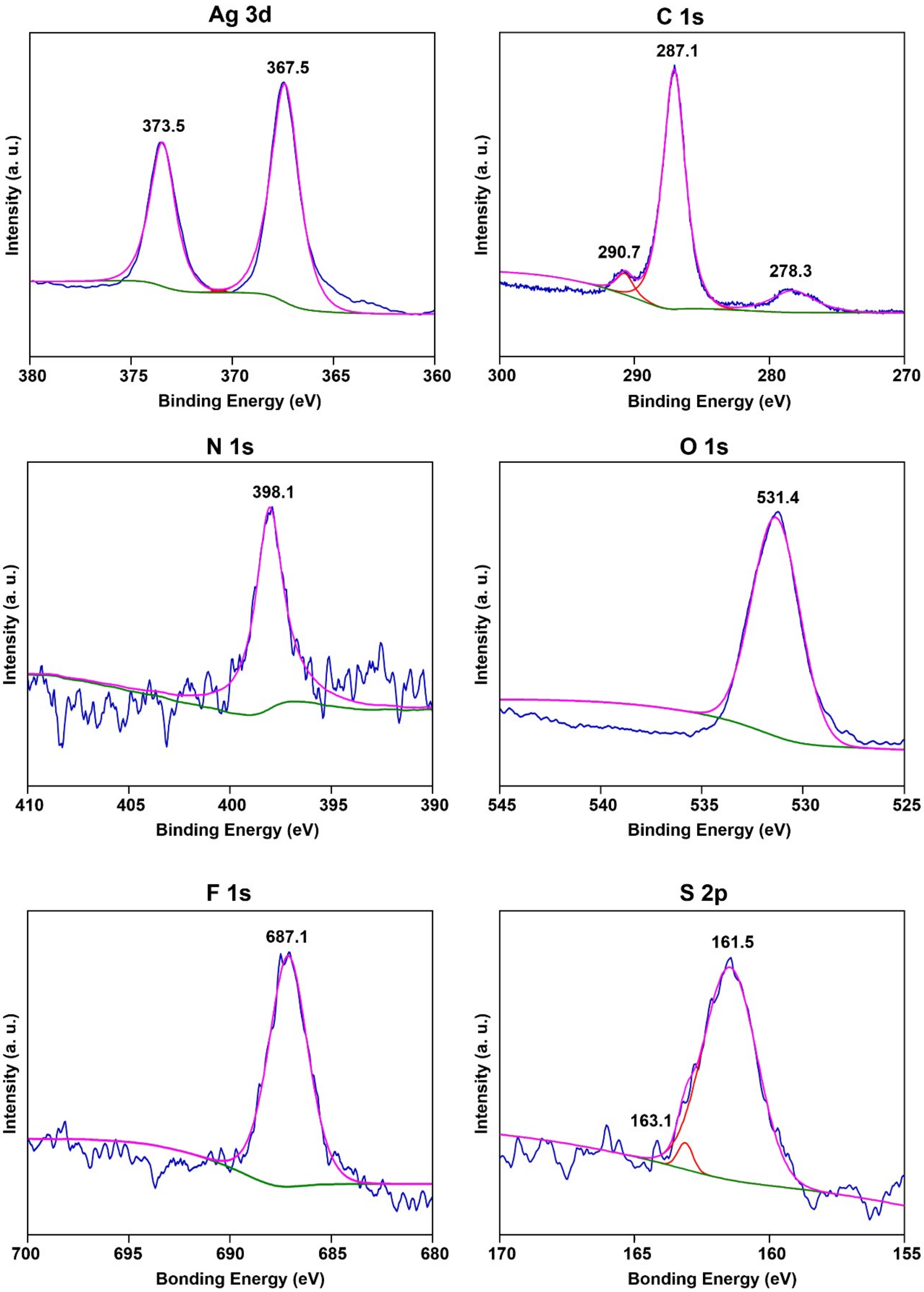

Fig. S7 High-resolution XPS binding energy spectrum of each element present in **TUS 2**.

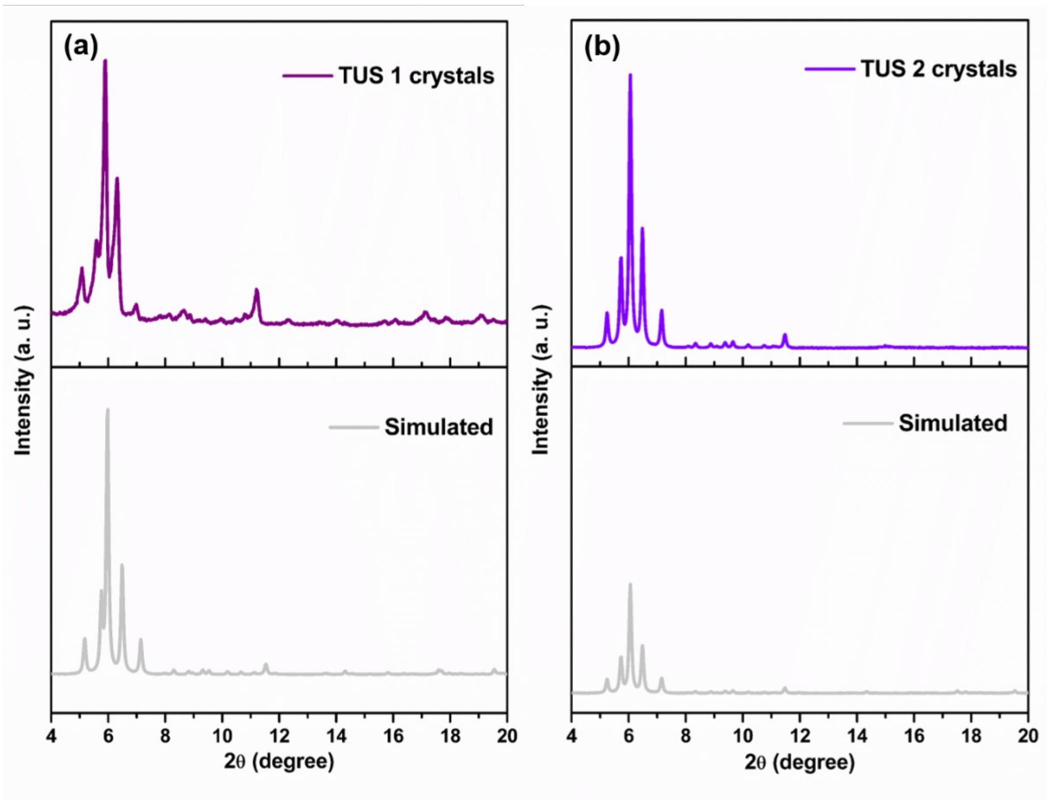

Fig. S8 Simulated and experimental PXRD patterns of **TUS 1** and **TUS 2** to check the purity of crystals.

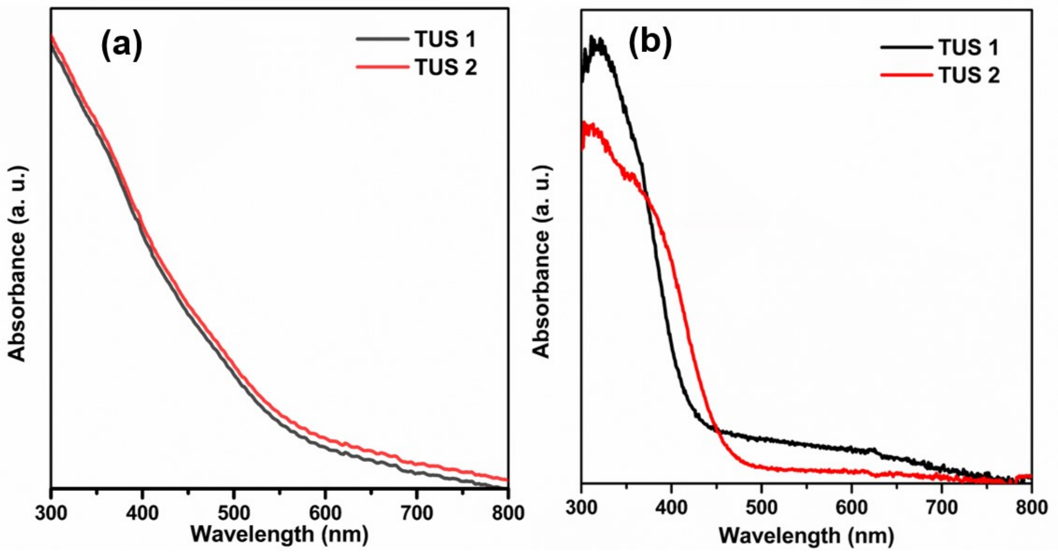

Fig. S9 (a) UV-Vis absorbance of **TUS 1** and **TUS 2** dispersing in water and (b) solid-state UV-Vis absorbance of **TUS 1** and **TUS 2**.

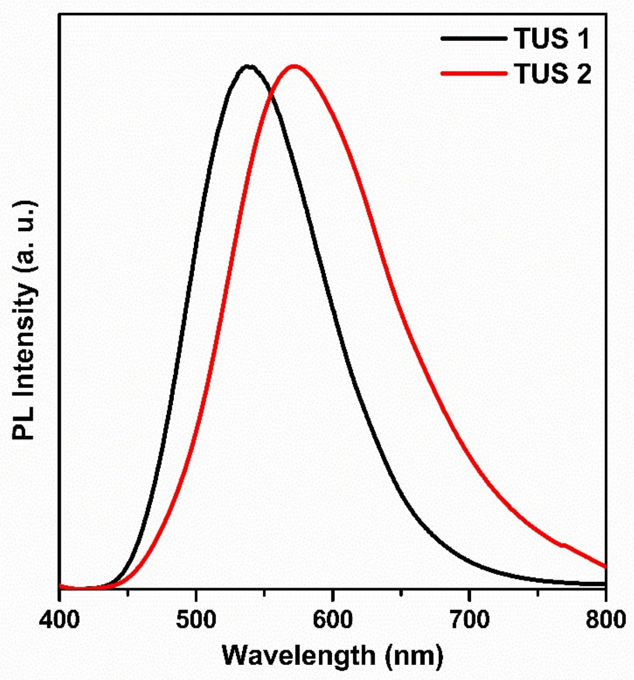

Fig. S10 Solid-state PL emission of both **TUS 1** and **TUS 2**.

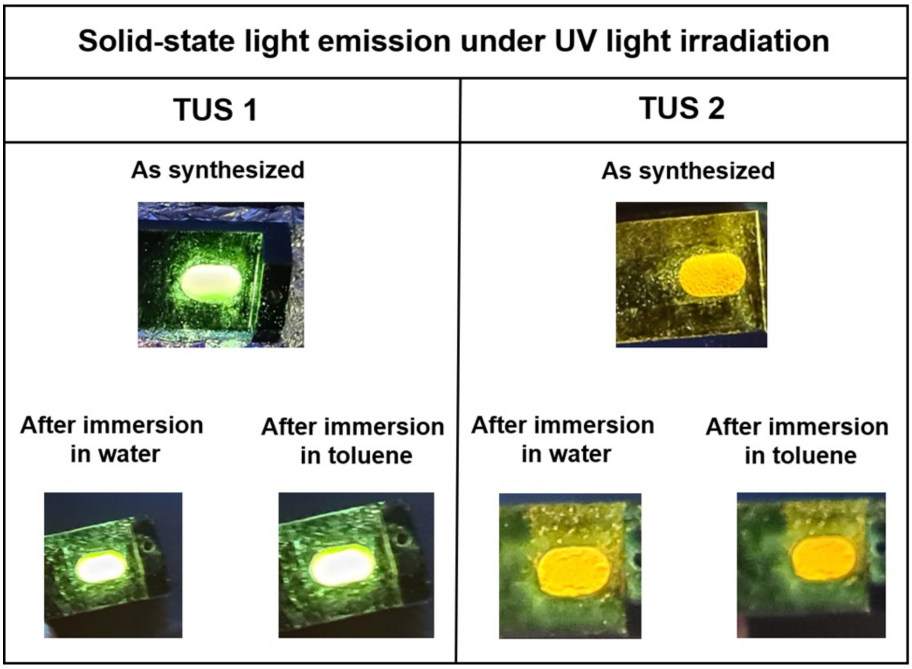

Fig. S11 Solid-state light emissions of both **TUS 1** and **TUS 2** under UV light irradiation before and after immersion in water and toluene.

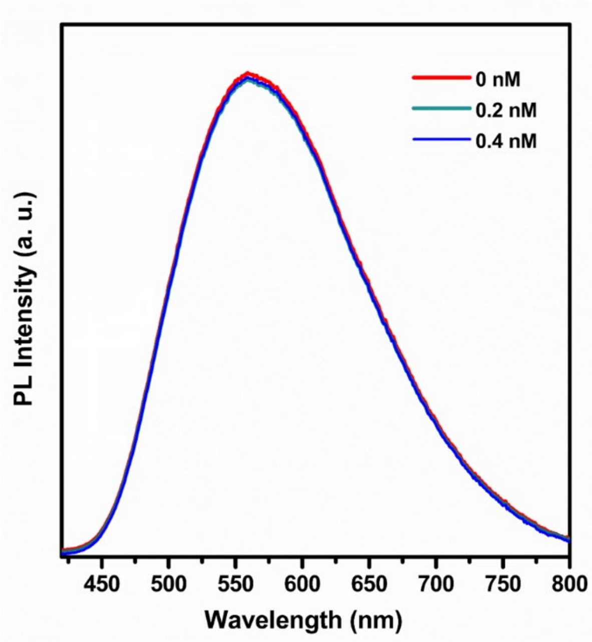

Fig. S12 Sensing of Fe^{3+} ions by **TUS 2** when the concentration is below 1 nM.

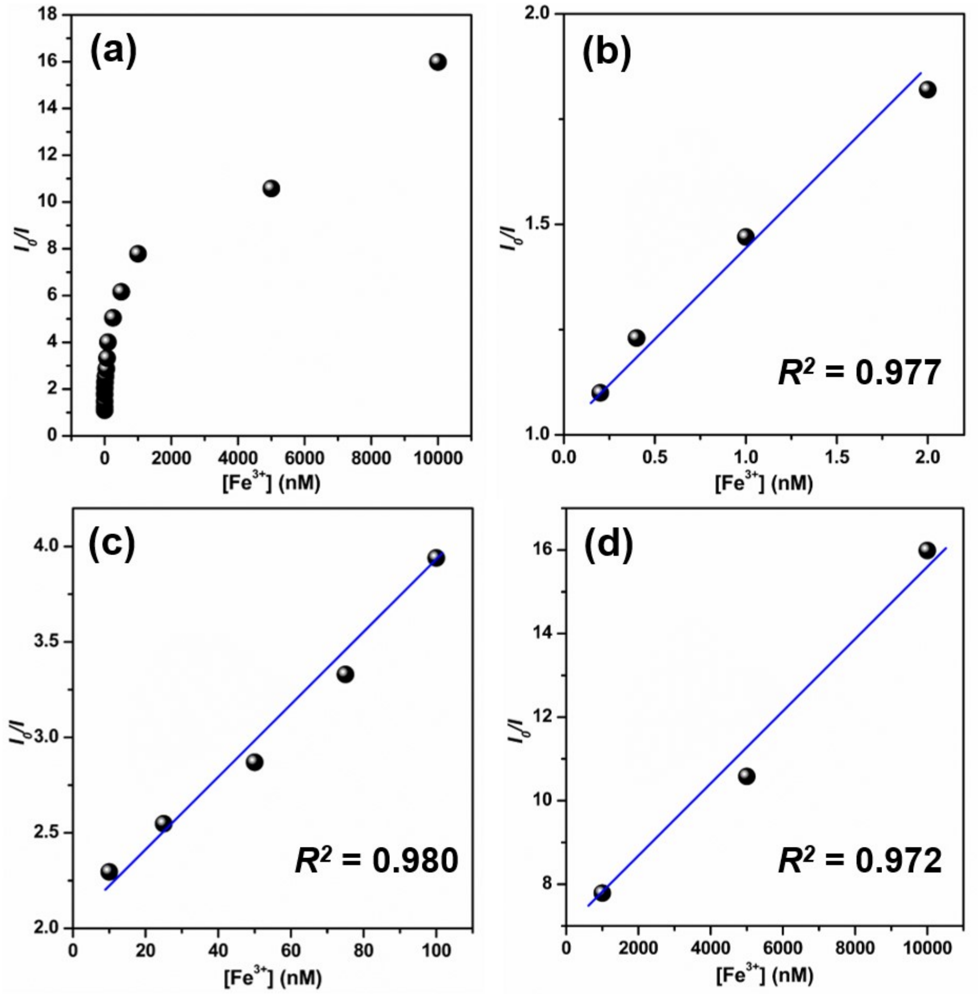

Fig. S13 (a) Relationship between the concentrations of Fe^{3+} and the PL intensities of **TUS 1**. (b), (c) and (d) represent the linear relationship in a short range of analyte concentration.

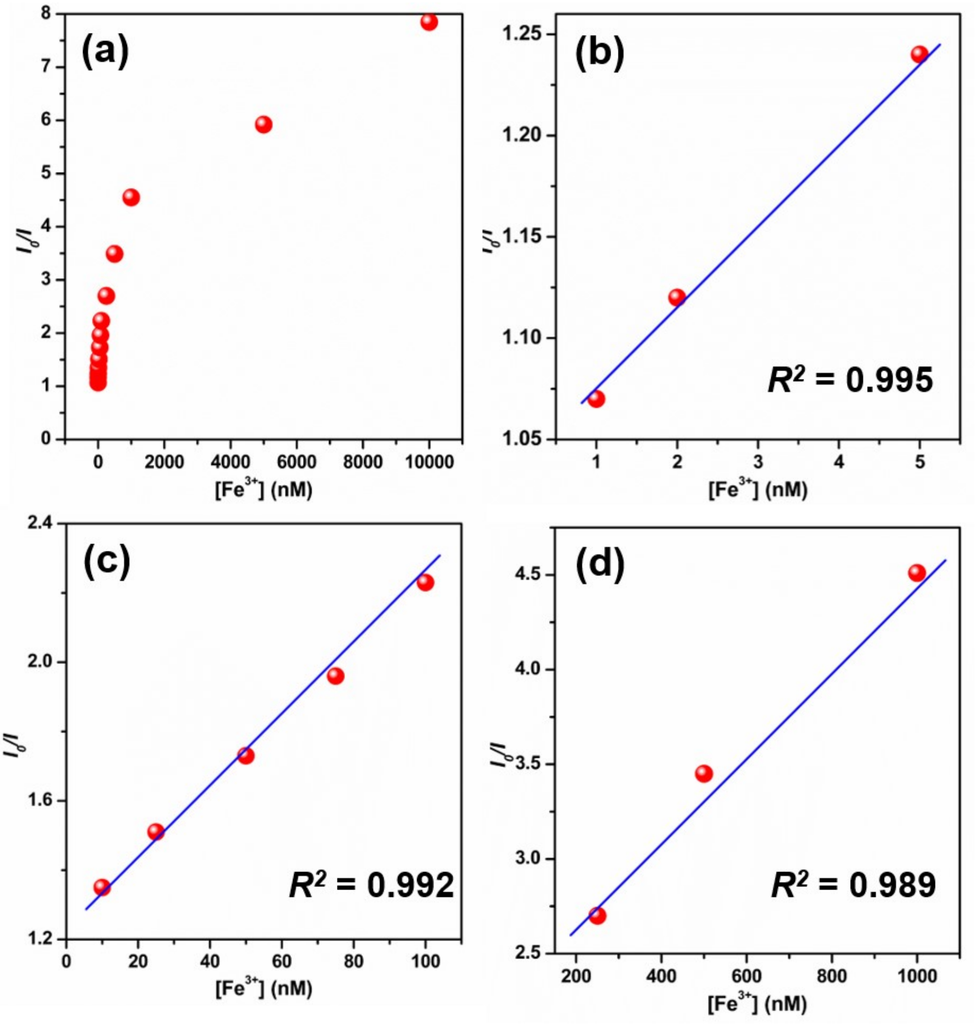

Fig. S14 (a) Relationship between the concentrations of Fe^{3+} and the PL intensities of **TUS 2**. (b), (c) and (d) represent the linear relationship in a short range of analyte concentration.

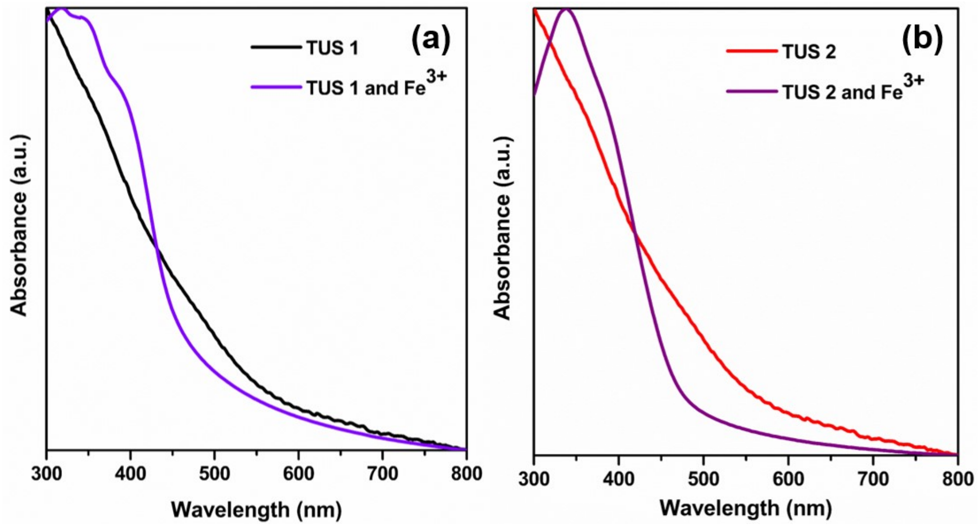

Fig. S15 Change in absorption after adding Fe^{3+} solution in (a) **TUS 1** and (b) **TUS 2**.

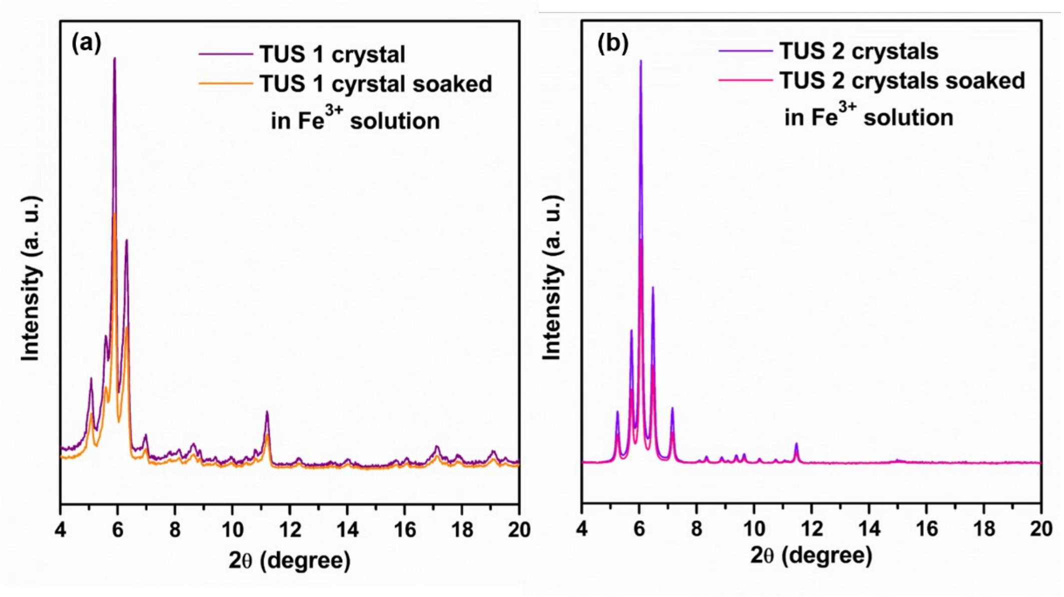

Fig. S16 PXRD patterns of (a) **TUS 1** and (b) **TUS 2** crystals before and after immersing in Fe^{3+} solution.

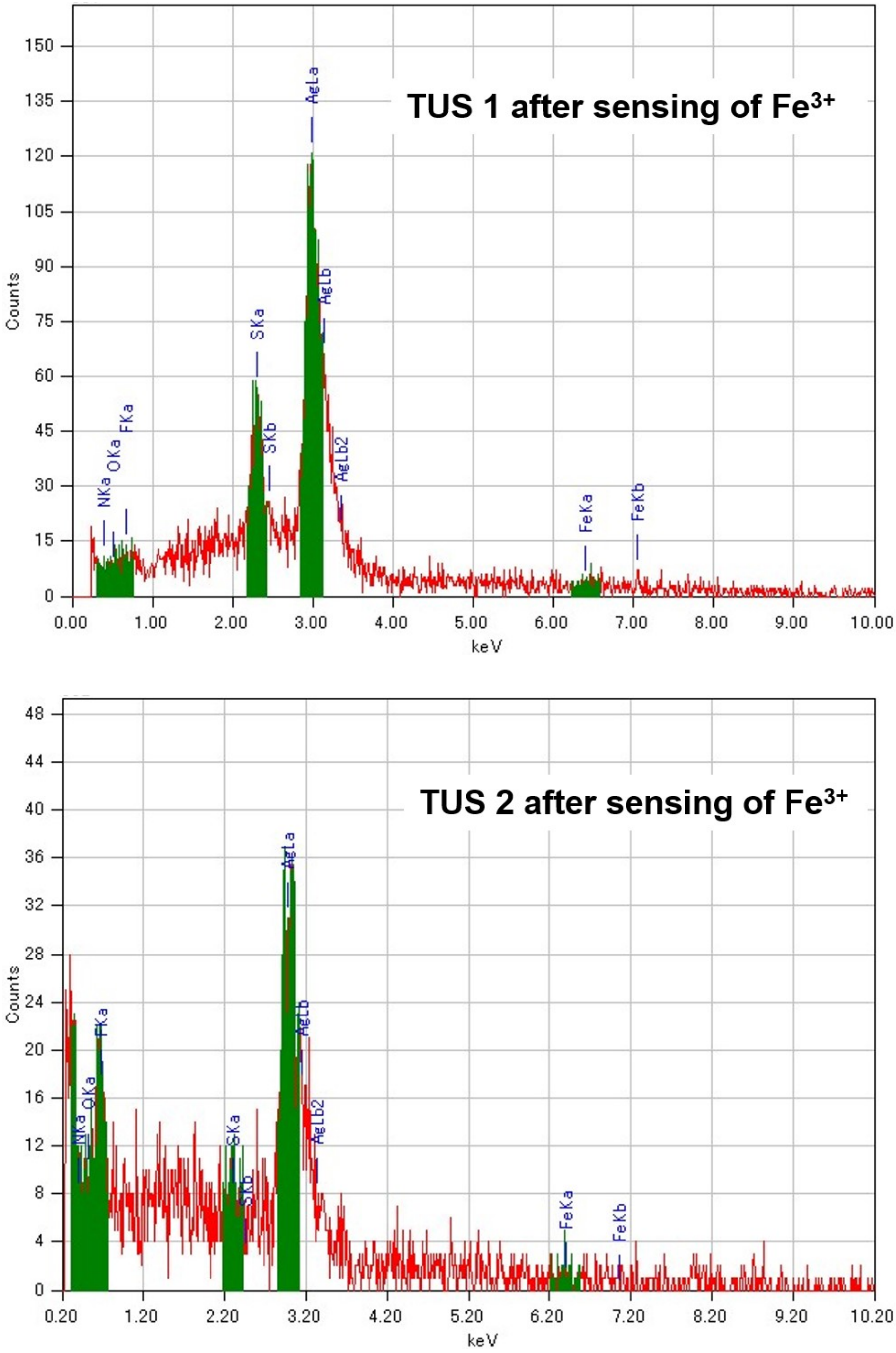

Fig. S17 EDS of both SCAMs after sensing of Fe^{3+}.

References

1. Bruker APEX3, v2019.1–0, Bruker AXS Inc., Madison, WI, USA, 2019.
2. B. K. Teo, Y. H. Xu, B. Y. Zhong, Y. K. He, H. Y. Chen, W. Qian, Y. J. Deng and Y. H. Zou, *Inorg. Chem.*, 2001, **40**, 6794-6801.
3. S. Das, T. Sekine, H. Mabuchi, S. Hossain, S. Das, S. Aoki, S. Takahashi and Y. Negishi, *Chem. Commun.*, 2023, **59**, 4000.